Comparing spectral models to predict manganese content in *Rosa* spp. leaves using VIS-NIR data

Comparación de modelos espectrales para predecir el contenido de manganeso en hojas de *Rosa* spp. usando datos VIS-NIR

Oscar Hernán Franco Montoya[1*] and Luis Joel Martínez Martínez[1]

ABSTRACT

This study, conducted on the Freedom rose cultivar grown under greenhouse conditions in the municipality of Tocancipá, Cundinamarca (Colombia), implemented Partial Least Squares Regression (PLSR) and Principal Component Regression (PCR) methods using visible and near-infrared (VIS-NIR) spectroradiometry from 350 to 2500 nm to predict manganese (Mn) content in rose leaves. A randomized complete block design (RCBD) with manganese doses of 0%, 25%, 50%, 75%, and 100% of the reference dose of 2 mg L^{-1} was established in 25 plots with five treatments and five replicates. Samplings were conducted in the five phenological stages of "palmiche", "rice", "chickpea", "scratch color", and "straight sepals", analyzing 10 plants per treatment, and spectral responses were measured on the adaxial leaf surface using the FieldSpec® 4 spectroradiometer. For model generation (PLSR and PCR), 24 predictive models were evaluated, comprising three spectral response ranges: range 1 (350-1000 nm), range 2 (350-1800 nm), and range 3 (350-2500 nm), applying different spectral correction methods: raw data (RD), Savitzky-Golay (SG), range normalization (RN), and Savitzky-Golay followed by range normalization (SG-RN). A total of 100 samples were used: 80 for calibration and 20 for external validation, randomly selected to represent the variability of the treatments. The spectral corrections improved the accuracy and robustness of the predictions, with the RN-PLSR and SG-RN-PLSR models showing the best performance metrics (R^2, RMSE, and RPD). The most relevant wavelengths were 523 nm, 557 nm, and around 720 nm, with correlations greater than 0.6 with the Mn concentration in leaves.

Key words: PLSR, PCR, crop nutrition, spectral reflectance, spectral smoothing, predictive models, multivariate analysis, spectroradiometer.

RESUMEN

Este estudio, realizado en cultivo de rosa variedad Freedom sembrada bajo invernadero en el municipio de Tocancipá, Cundinamarca (Colombia), implementó métodos de Regresión por Mínimos Cuadrados Parciales (RMCP) y Regresión con Componentes Principales (RCP) utilizando espectroradiometría visible e infrarroja cercana (VIS-NIR) de 350 a 2500 nm para predecir el contenido de manganeso (Mn) en hojas de rosa. Se estableció un diseño de bloques completos al azar (BCA) con dosis de manganeso de 0%, 25%, 50%, 75% y 100% (referencia de 2 mg L^{-1}) en 25 parcelas con cinco tratamientos y cinco repeticiones. Se realizaron muestreos en los cinco estados fenológicos "palmiche", "arroz", "garbanzo", "rayando color" y "sépalos rectos", analizando 10 plantas por tratamiento; las respuestas espectrales se midieron en la superficie adaxial de las hojas utilizando el espectroradiómetro FieldSpec® 4. Para la generación de los modelos (RMCP y RCP), se evaluaron 24 modelos predictivos conformados por tres rangos de respuesta espectral: rango 1 (350-1000 nm), rango 2 (350-1800 nm) y rango 3 (350-2500 nm), aplicando diferentes métodos de corrección de espectro: datos crudos (RD), Savitzky-Golay (SG), normalización por rangos (NR) y Savitzky-Golay seguido de normalización por rangos (SG-NR); se usaron 100 muestras en total: 80 para calibración y 20 para validación externa, seleccionadas aleatoriamente para representar la variabilidad de los tratamientos. Las correcciones del espectro mejoraron la precisión y solidez de la predicción, siendo los modelos NR-PLSR y SG-NR-PLSR los que presentaron las mejores valoraciones en las métricas (R^2, RMSE y RDP), mientras que las longitudes de onda más relevantes fueron 523 nm, 557 nm y cerca de 720 nm, con correlaciones superiores a 0,6 con la concentración de Mn en hojas.

Palabras clave: RMCP, RCP, nutrición de cultivos, reflectancia espectral, suavizado espectral, modelos predictivos, análisis multivariado, espectroradiómetro.

Introduction

The rose (*Rosa* spp.) is one of the most economically important cut flowers worldwide and holds a particularly prominent place in Colombia's agricultural exports. Introduced in the country during the 1960s through a partnership between foreign investors and local entrepreneurs, rose cultivation rapidly expanded, finding ideal agroecological

Received for publication: January 15, 2025. Accepted for publication: April 30, 2025. Doi: 10.15446/agron.colomb.v43n1.118322

[1] Universidad Nacional de Colombia, Facultad de Ciencias Agrarias, Bogotá (Colombia).
* Corresponding author: ohfrancom@unal.edu.co

conditions in the departments of Cundinamarca and Antioquia (Arbeláez, 1993). Today, Colombia is the leading exporter of flowers in Latin America and the second largest globally, surpassed only by the Netherlands. Roses account for nearly 48% of the total area dedicated to flower production, making them the primary species cultivated. This industry generates over 120,000 direct jobs and approximately 99,000 indirect jobs, with significant participation from women (ICA, 2024). The continued growth of rose exports and increasing international market demands (related to stem uniformity, bud size, color intensity, and harvest stage consistency) highlight the need for precise crop management and the implementation of advanced technological tools for quality optimization (Ruppenthal & Conte, 2005).

Manganese (Mn) is an essential nutrient for the growth and development of rose crops, participating in key physiological processes such as photosynthesis. Mn is a cofactor in at least 35 metabolic processes, playing a crucial role in chlorophyll formation, oxygen evolution in photosystem II, and redox reactions within the electron transport chain during photosynthesis (Rashed *et al*., 2019). It also acts as an activator of enzymes involved in respiration, amino acid synthesis, and hormonal regulation (Santos *et al*., 2017).

However, both manganese deficiency and excess can have negative effects on plants. Mn deficiency in plants interferes with photosynthesis, affecting photolysis in photosystem II and damaging chloroplasts, which impedes proper electron production for the process. On the other hand, excess manganese can be toxic, and tolerance to its toxicity varies depending on the species and genotype of the plant (Humphries *et al*., 2006; Santos *et al*., 2017). In rose plants, manganese is present in low concentrations at the foliar level and is a relatively immobile nutrient, meaning it does not easily relocate from older leaves, leading to a deficiency in expanding young leaves (Humphries *et al*., 2006). Therefore, deficiency symptoms are not evident in older leaves or in young leaves that have not yet fully expanded. This may indicate a higher demand in these developing leaves, or it may simply be a matter of source-sink dynamics favoring the faster-growing tissues (Humphries *et al*., 2006).

The diagnosis of nutritional status in rose cultivation is essential for making informed decisions about the application of exogenous fertilizers, which can be mainly administered through the fertigation system or, to a lesser extent, by foliar application. Fertilizer formulations must be applied at the right time, considering the interactions between soil/substrate, plants, and water, as these factors directly affect the quality and productivity of the crop, which are fundamental for its sustainability. An adequate supply of micronutrients, such as manganese, can significantly increase crop productivity, making it essential to maintain proper nutritional balance through timely diagnostics (Hariyadi *et al*., 2019). In flower crops, traditional nutritional analysis requires destructive methods, which are slow and resource-intensive, causing delays in diagnosis. For this reason, there has been an increased interest in developing faster, non-destructive alternative methods, such as the use of sensors. In this context, reflectance measurement has emerged as a promising alternative for characterizing the nutritional status of plants, allowing for a quicker and more efficient estimation of key parameters at the foliar level. This approach presents a valuable tool for improving nutritional diagnostics in rose cultivation.

Numerous studies have linked the chemical composition of plants with the absorption of electromagnetic radiation. This relationship has evolved from laboratory near-infrared spectroscopy (NIRS) research to remote sensing, where it has been shown that biochemical concentrations of elements such as nitrogen in foliar tissue are closely related to radiation through spectral absorption features, both in dry and fresh leaves. However, fresh leaves are influenced by water content, which alters their absorption characteristics in the near-infrared region of the spectrum (1000–2500 nm) (Huber *et al*., 2008). The reflectance of leaves exhibits specific characteristics: in general, pigments present in the leaves have a significant influence on reflectance in the visible region, while cellular structure manifests in near-infrared reflectance. Additionally, proteins and water content primarily respond in the near-infrared to mid-infrared regions (Liang, 2005).

In recent years, significant progress has been made in developing spectral-based models for predicting micronutrient concentrations in plants. For example, Yu *et al*. (2019) demonstrated the high potential of near-infrared spectroscopy (NIRS) combined with chemometric techniques to predict manganese content in cottonseed flour. The study applied spectral corrections such as standard normal variate (SNV) and first derivative (FD), along with advanced variable selection methods like Monte Carlo uninformative variable elimination (MCUVE) and successive projections algorithm (SPA). The resulting models yielded high prediction accuracy, with RMSEP = 1.99, R^2 = 0.95, and RPD = 4.37, confirming the effectiveness of optimized spectral preprocessing and variable selection in enhancing model robustness.

Similarly, Boshkovski *et al*. (2020) assessed nutrient dynamics in common bean plants subjected to abiotic stress using spectral reflectance and multivariate regression. Their findings revealed significant correlations between reflectance and several nutrients, including manganese, boron, iron, phosphorus, and zinc, as well as vegetation indices like NDVI. Custom spectral indices developed in the study exhibited strong predictive power for a wide range of macro- and micronutrients. Additionally, Santoso *et al*. (2019) evaluated nutrient content in oil palm leaves using reflectance data and built predictive models through stepwise regression and principal component regression (PCR). The models achieved moderately high R^2 values, ranging from 0.33 to 0.53, particularly for nitrogen and calcium, demonstrating the potential of VIS-NIR data in estimating leaf nutrient status in tropical crops.

Other researchers used hyperspectral spectroscopy to develop spectral indices and multivariate models, combined with machine learning, to predict foliar nutrients in mango. The results showed that conventional models such as partial least squares regression (PLSR) and principal component regression (PCR), were ineffective in predicting the nutrients. However, models combining PLSR with machine learning techniques, such as the Cubist model, support vector regression (SVR), and elastic net, showed good performance, especially in predicting nitrogen, phosphorus, potassium, zinc, magnesium, and sulfur. The results suggest that hyperspectral remote sensing has great potential for non-destructive estimation of foliar nutrients in mango, contributing to more precise nutrient management (Mahajan *et al*., 2021).

In a related study on citrus, a calibration model based on spectroscopy was developed to predict the foliar concentrations of macro and micronutrients in *Citrus clementina* plantations using fast, non-destructive spectral measurements. The results showed that spectroscopy, using a portable spectrometer to measure spectral absorbance (430–1040 nm), effectively estimated nutrient levels, with determination coefficients ranging from 0.31 to 0.69, with the highest values observed for phosphorus (P), potassium (K), and boron (B). Similarly, the technique showed high potential for rapid and non-destructive prediction of foliar nutrients, reinforcing the idea that hyperspectral remote sensing is a promising tool for nutrient management in crops (Acosta *et al*., 2023).

Similarly, in oil palm plantations, spectral reflectance was used to predict key nutrients such as nitrogen, phosphorus, potassium, calcium, magnesium, boron, copper, and zinc. In the study, the proposed vegetation indices performed better than conventional indices, and multivariate models based on principal component regression (PCR) were more effective when significant variables selected through stepwise regression were used, with wavelengths in the green region contributing the most to the model (Santoso *et al*., 2019). Together, these studies demonstrate the great potential of spectral remote sensing to predict foliar nutrients in various crops, facilitating more precise nutrient management in agriculture. In this context, the present research evaluated the potential of reflectance data, obtained in the range of 350 nm to 2500 nm using a spectroradiometer, in rose crops planted under greenhouse conditions. The aim was to develop predictive models based on spectral responses to estimate the foliar manganese content in rose crops, using partial least squares regression (PLSR) and principal component regression (PCR) analysis.

In this context, the nutritional management of rose crops not only directly impacts flower quality but also the country's competitiveness in international markets. However, traditional methods for nutritional diagnosis are destructive, time-consuming, and costly, which delays timely decision-making in the field. In response to this challenge, rapid and non-destructive tools such as visible and near-infrared (VIS-NIR) spectroradiometry have gained relevance, as they allow for the characterization of plant nutritional status through spectral response. Although this technology has shown promising results in other crops, its application in roses remains limited. Therefore, this study aims to contribute to the knowledge of spectral multivariate modeling for predicting foliar manganese content in *Rosa* spp., supporting the development of more efficient monitoring systems adapted to tropical production conditions and with potential for implementation in the Colombian floriculture industry.

Materials and methods

Experimental design

The study was conducted in a greenhouse located in Tocancipá, Cundinamarca (Colombia), at 2,605 m a.s.l. (4°58'40.1" N, 73°59'06.6" W), using *Rosa* spp. (Freedom cultivar). The experimental area comprised 176 m^2, divided into 25 plots of 1.35 m^2 (0.3 m × 4.5 m), each containing 60 plants. A randomized complete block design (RCBD) was implemented to minimize environmental variability within the greenhouse. The experimental unit consisted of one plot (60 plants); five manganese (Mn) treatments were applied at concentrations of 0%, 25%, 50%, 75%, or 100%

of the reference dose 2 mg L^{-1} Mn-EDTA, each replicated five times across blocks (hydroponic banks). The response variable was foliar Mn concentration, and the explanatory variables were spectral reflectance values collected at different phenological stages.

Nutrient solutions were supplied through a drip fertigation system, maintaining a pH between 5.3 and 5.8 and electrical conductivity between 1.5 and 1.8 dS m^{-1}. The other macro- and micronutrients were kept constant in the nutrient solution across treatments (Tab. 1).

All treatments received the same concentrations of macronutrients and micronutrients, except for manganese (Mn), which was applied in increasing doses. Nutrient solutions were prepared to ensure consistency across treatments, minimizing confounding effects in the evaluation of Mn-specific responses.

Plant material and sample processing

The samplings were conducted across five key phenological stages: "palmiche", "rice", "chickpea", "scratch color", and "straight sepals" (Franco Montoya & Martínez Martínez, 2024). For each stage, 10 fully developed leaves were sampled from each plot. The same leaves were used for both spectral measurements and chemical analysis to ensure consistency.

Samples were stored in a cooler and transported to the laboratory within 5 h after collection. Leaves were kept refrigerated (4°C) until processing. Manganese content was determined using microwave-assisted digestion (HNO_3 + H_2O_2), followed by analysis with inductively coupled plasma optical emission spectroscopy (ICP-OES). The standard error of the laboratory method for Mn determination was 0.09 mg kg^{-1} (Ghosh *et al*., 2013).

Spectral measurement

Spectral data were collected using a FieldSpec® 4 spectroradiometer (Malvern Panalytical, UK), which covers a wavelength range from 350 to 2,500 nm. The device has a wavelength accuracy of 0.5 nm, a spectral resolution of <3.0 nm at 700 nm, and a noise-equivalent radiance of 5 × 10^{-10} W/cm^2/nm/sr at 700 nm. It records data across 2,151 spectral channels and weighs approximately 5.44 kg (12 lbs).

Measurements were taken on the adaxial surface of the fourth and fifth fully developed leaves using a leaf clip accessory equipped with an internal halogen light source and an integrated Spectralon® white reference. For each leaf, five reflectance scans were taken and averaged. All measurements were conducted under controlled lighting conditions at the Geomatics Laboratory of the Universidad Nacional de Colombia.

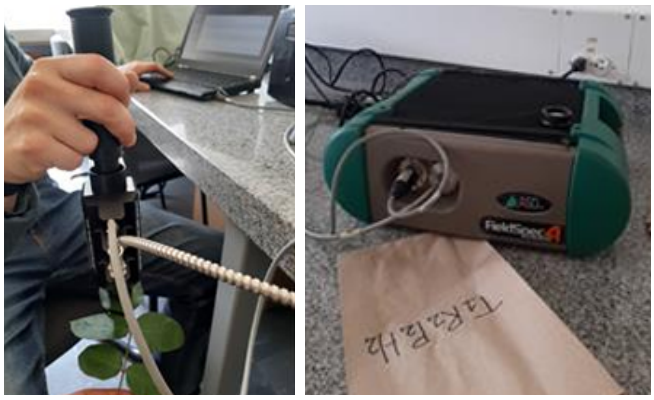

FIGURE 1. Capturing spectral responses: A) Leaf clip accessory, B) FieldSpec 4® spectroradiometer.

Spectral preprocessing and modeling

A total of 100 samples were used to build prediction models: 80 for calibration and 20 for external validation, selected randomly to represent treatment variability. Three spectral ranges were analyzed: 350–1000 nm, 350–1800 nm, and 350–2500 nm. Four preprocessing techniques were applied:

- Raw data (RD);
- Savitzky-Golay smoothing (SG) with a window of 15 points and a second-order polynomial;
- Range normalization (RN);
- SG followed by RN (SG-RN).

TABLE 1. Nutrient composition of the fertigation solution for each manganese (Mn) treatment.

Treatments	(Mn supply, % of the reference dose)	N	P	K	Ca	Mg	S	Mn	Zn	Cu	Fe	B	Mo
		mg L^{-1}											
T1	0%	160	10	180	100	40	14	0	0.7	1.2	2	0.2	0.1
T2	25%	160	10	180	100	40	14	0.5	0.7	1.2	2	0.2	0.1
T3	50%	160	10	180	100	40	14	1	0.7	1.2	2	0.2	0.1
T4	75%	160	10	180	100	40	14	1.5	0.7	1.2	2	0.2	0.1
T5	100%	160	10	180	100	40	14	2	0.7	1.2	2	0.2	0.1

Predictive models were developed using Partial Least Squares Regression (PLSR) and Principal Component Regression (PCR). All analyses were conducted in R software (version 10.0.19045.5487), employing a set of specialized packages for data preprocessing, modeling, and visualization. The following R packages were used: pls, caret, signal and pracma, tidyverse, including dplyr, tidyr, and ggplot2, and lattice.

Model performance was assessed based on the coefficient of determination (R^2), root mean square error of prediction (RMSEP), and residual predictive deviation (RPD).

Results and discussion

Figure 2 shows that the foliar Mn concentration in rose plants varied according to the fertigation applications, indicating that the leaves respond directly to the amount of Mn supplied. In the first sampling, the treatments showed similar Mn concentrations, except for the 0% reference dose treatment T1, which had the lowest value. From the second sampling onward, differences in concentrations were observed, suggesting that Mn accumulation in the foliar tissue depends on its availability in the substrate and the plant response to fertilization applications. In summary, rose leaves accumulate Mn according to the supplied concentration, reflecting a direct response to the fertilization levels.

Table 2 presents the results obtained at different phenological stages, highlighting the best models according to the evaluated prediction metrics. In the palmiche phenological stage, the most accurate model was obtained using the spectral responses from the 350 nm to 1000 nm range, applying Savitzky-Golay smoothing with 15 points and range normalization. This model achieved an RPD of 1.24, an R^2 of 0.36, and an RMSE of 14.37. In the rice phenological stage, the best model was generated using the PLSR technique with raw values in the 350 nm to 2500 nm range, yielding the best results without the need for spectral correction. In the chickpea phenological stage, the standout model was the RN-PLSR in the 350 nm to 1000 nm range, with an RPD of 2.01. This model presented an R^2 of 0.67 and an RMSE of 10.70, with good performance for the evaluated metrics. In the scratch color phenological stage, the best model was obtained using the 350 nm to 1800 nm range, applying the Savitzky-Golay smoothing algorithm and range normalization with the PLSR technique (SG-RN-PLSR). This model showed metric values with an RPD of 1.73, an R^2 of 0.66, and an RMSE of 19.33. Finally, the straight sepals phenological stage showed the best results in terms of RPD, with a model based on the 350 nm to 2500 nm range with the RD-PLSR. This model achieved an RPD of 3.05, an R^2 of 0.88, and an RMSE of 14.66, standing out for its high performance compared to other phenological stages.

In summary, the phenological stages of straight sepals and chickpea stood out for presenting the best values in the evaluated metrics, especially RPD, suggesting that the methodology used at these phenological stages is particularly effective. The straight sepals stage, with an RPD of 3.05, showed the best overall performance, making it recommended for future research and spectral modeling applications, as it provides more accurate and consistent results. The chickpea phenological stage also showed high

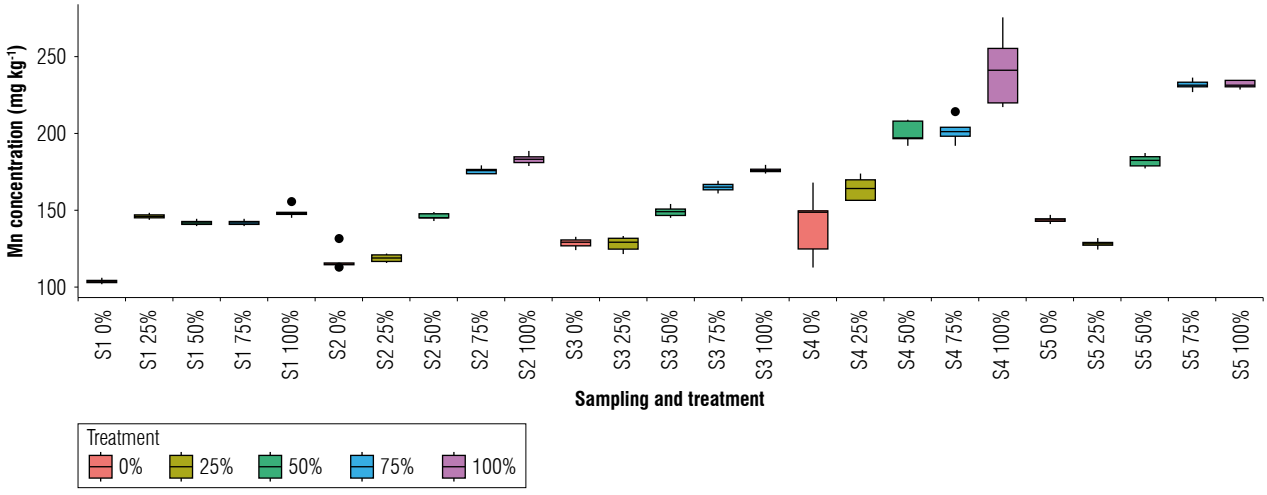

FIGURE 2. Foliar Mn concentration (mg kg^{-1}) in rose plants at five phenological stages: S1, palmiche; S2, rice; S3, chickpea; S4, scratch color; S5, straight sepals. Treatments – Mn supply, % of the reference dose.

TABLE 2. Results of the evaluated metrics for the predictive models.

Palmiche						Rice						Chickpea					
Model	**Range(nm)**	**F**	**R^2**	**RMSE**	**RPD**	**Model**	**Range(nm)**	**F**	**R^2**	**RMSE**	**RPD**	**Model**	**Range(nm)**	**F**	**R^2**	**RMSE**	**RPD**
SG-RN-PLSR	350-1000	7	0.36	14.37	1.24	RD-PLSR	350-2500	4	0.63	16.79	1.66	RN-PLSR	350-1000	6	0.67	10.70	2.01
RD-PLSR	350-1800	4	0.36	14.23	1.24	SG-PLSR	350-2500	3	0.62	16.91	1.64	SG-RN-PLSR	350-1000	6	0.66	10.94	1.98
SG-PLSR	350-1800	4	0.33	14.25	1.23	RD-PCR	350-2500	4	0.59	17.54	1.58	RN-PLSR	350-1800	7	0.73	9.75	1.96
SG-RN-PLSR	350-1800	3	0.29	14.75	1.20	SG-PCR	350-2500	4	0.59	17.54	1.58	SG-PLSR	350-1000	6	0.63	11.33	1.91
SG-RN-PCR	350-1800	4	0.27	14.95	1.20	SG-RN-PLSR	350-1000	7	0.26	23.68	1.32	RD-PLSR	350-1000	6	0.63	11.42	1.90
RN-PLSR	350-1800	3	0.28	14.78	1.20	RN-PCR	350-2500	4	0.42	21.01	1.31	RD-PCR	350-1800	6	0.72	10.09	1.87
RD-PCR	350-1800	7	0.28	15.22	1.16	SG-RN-PCR	350-2500	4	0.42	21.02	1.31	SG-PLSR	350-1800	7	0.75	9.43	1.87
RN-PCR	350-1800	5	0.23	15.28	1.15	RN-PLSR	350-2500	3	0.41	21.06	1.31	SG-PCR	350-1800	6	0.71	10.11	1.87
RN-PCR	350-2500	4	0.10	15.84	1.06	SG-RN-PLSR	350-2500	3	0.41	21.09	1.31	SG-RN-PLSR	350-1800	7	0.73	9.75	1.84
SG-RN-PCR	350-2500	4	0.10	15.84	1.06	RD-PLSR	350-1000	6	0.30	23.08	1.27	SG-RN-PCR	350-1800	6	0.70	10.30	1.84
RN-PLSR	350-1000	4	0.09	16.84	1.05	RN-PLSR	350-2500	4	0.36	22.07	1.25	RN-PCR	350-1800	6	0.70	10.39	1.83
SG-PCR	350-1800	1	0.08	16.78	1.04	SG-RN-PLSR	350-2500	4	0.36	22.07	1.25	RD-PLSR	350-2500	7	0.63	11.92	1.66
RD-PLSR	350-1000	4	0.04	17.67	0.99	RN-PLSR	350-1000	6	0.17	25.08	1.22	RD-PLSR	350-1800	7	0.75	9.47	1.66
SG-PLSR	350-1000	4	0.04	17.68	0.99	RD-PLSR	350-2500	3	0.32	22.69	1.21	RN-PLSR	350-2500	7	0.61	12.38	1.60
RD-PCR	350-2500	1	0.00	16.83	0.99	SG-PLSR	350-2500	4	0.32	22.70	1.21	SG-RN-PLSR	350-2500	5	0.57	12.87	1.53
SG-PCR	350-2500	1	0.00	16.83	0.99	SG-RN-PCR	350-2500	5	0.31	22.78	1.21	SG-PLSR	350-2500	5	0.51	13.80	1.44
RN-PCR	350-1000	5	0.02	17.77	0.99	RD-PCR	350-2500	5	0.23	24.11	1.14	RD-PCR	350-1000	3	0.44	13.95	1.40
SG-RN-PCR	350-1000	5	0.01	17.81	0.99	SG-PCR	350-2500	5	0.37	24.11	1.14	SG-PCR	350-1000	3	0.44	13.95	1.40
SG-PCR	350-1000	4	0.02	18.05	0.97	SG-RN-PCR	350-1000	6	0.11	26.00	1.13	SG-RN-PCR	350-1000	2	0.40	14.45	1.34
RD-PCR	350-1000	4	0.02	18.06	0.97	SG-PLSR	350-1000	2	0.15	25.37	1.13	RN-PCR	350-1000	2	0.40	14.47	1.33
SG-RN-PLSR	350-2500	6	0.14	17.80	0.94	RN-PCR	350-1000	6	0.10	26.11	1.12	RD-PCR	350-2500	5	0.23	17.30	1.14
RN-PLSR	350-2500	6	0.14	17.87	0.94	SG-PCR	350-1000	1	0.11	26.07	1.10	SG-PCR	350-2500	5	0.23	17.30	1.14
SG-PLSR	350-2500	7	0.12	18.31	0.91	RD-PCR	350-1000	1	0.11	26.07	1.10	RN-PCR	350-2500	4	0.13	18.39	1.08
RD-PLSR	350-2500	7	0.12	18.37	0.91	RN-PCR	350-2500	1	0.16	25.16	1.09	SG-RN-PCR	350-2500	4	0.11	18.58	1.07

Scratch color						Straight sepals					
Model	**Range(nm)**	**F**	**R^2**	**RMSE**	**RPD**	**Model**	**Range(nm)**	**F**	**R^2**	**RMSE**	**RPD**
SG-RN-PLSR	350-1800	7	0.66	19.33	1.73	RD-PLSR	350-2500	6	0.88	14.661	3.05
RN-PLSR	350-1800	7	0.65	19.54	1.69	RN-PLSR	350-2500	5	0.84	17.213	2.54
RN-PLSR	350-1000	6	0.48	27.60	1.41	SG-PLSR	350-2500	5	0.84	17.349	2.53
SG-RN-PLSR	350-1000	6	0.46	27.93	1.39	SG-RN-PLSR	350-2500	5	0.83	17.806	2.47
SG-RN-PLSR	350-2500	7	0.37	29.03	1.27	RN-PCR	350-2500	2	0.65	25.499	1.69
RN-PLSR	350-2500	7	0.36	29.18	1.26	SG-RN-PCR	350-2500	2	0.65	25.584	1.68
RD-PLSR	350-1800	2	0.30	27.47	1.21	RD-PCR	350-2500	3	0.62	26.48	1.66
SG-PLSR	350-1800	2	0.30	27.47	1.21	SG-PCR	350-2500	3	0.62	26.481	1.66
RD-PCR	350-1800	2	0.29	27.74	1.20	RN-PCR	350-1800	2	0.53	30.493	1.46
SG-PCR	350-1800	2	0.29	27.74	1.20	SG-PLSR	350-1800	3	0.35	36.058	1.32
RD-PLSR	350-1000	5	0.30	31.97	1.19	RD-PLSR	350-1800	3	0.35	36.058	1.32
SG-PLSR	350-1000	5	0.30	31.97	1.19	RD-PCR	350-1800	3	0.34	36.303	1.31
RD-PCR	350-1000	6	0.24	33.18	1.15	SG-PCR	350-1800	3	0.34	36.304	1.31
SG-PCR	350-1000	6	0.24	33.20	1.15	RN-PLSR	350-1800	2	0.29	37.618	1.25
RN-PCR	350-2500	2	0.22	32.31	1.13	SG-RN-PLSR	350-1800	2	0.28	37.673	1.24
SG-RN-PCR	350-2500	2	0.21	32.33	1.13	SG-RN-PCR	350-1800	2	0.28	37.796	1.24
RN-PCR	350-1000	1	0.18	34.49	1.12	RD-PCR	350-1000	4	0.31	36.815	1.21
SG-RN-PCR	350-1000	1	0.18	34.53	1.11	SG-PCR	350-1000	4	0.31	36.822	1.21
RN-PCR	350-1800	2	0.16	30.15	1.09	RD-PLSR	350-1000	3	0.29	37.434	1.19
SG-RN-PCR	350-1800	2	0.15	30.40	1.08	SG-PLSR	350-1000	3	0.29	37.435	1.19
RD-PLSR	350-2500	2	0.04	35.79	1.02	RN-PCR	350-1000	4	0.22	39.253	1.16
SG-PLSR	350-2500	2	0.04	35.80	1.02	SG-RN-PCR	350-1000	4	0.22	39.261	1.15
RD-PCR	350-2500	2	0.19	36.65	1.00	RN-PLSR	350-1000	2	0.18	40.171	1.15
SG-PCR	350-2500	2	0.19	36.65	1.00	SG-RN-PLSR	350-1000	2	0.18	40.175	1.14

Factors: R^2, coefficient of determination; RMSE, root mean square error; RPD, residual predictive deviation.

performance, especially in models with R^2 values above 0.7 and RPD values close to 2.0, indicating that the methodology is suitable for predicting manganese content in rose plants.

Figure 3 presents the prediction results according to the reference data for the best-performing models in each of the evaluated phenological stages, using 20 validation data points per stage. In the case of the palmiche and rice phenological stages, since the values of their metrics do not show good performance, this methodology is not recommended. In contrast, starting from the chickpea phenological stage, the models show better performance according to their validation metrics. In the chickpea stage, an R^2V of 0.44, RMSEV of 14.68, and RPD of 2.0 were obtained; for the scratch color phenological stage, an R^2V of 0.85, RMSEV of 28.82, and RPD of 1.73 were obtained; and for the straight sepals stage, an R^2V of 0.69, RMSEV of 23.61, and RPD of 3.05 were obtained.

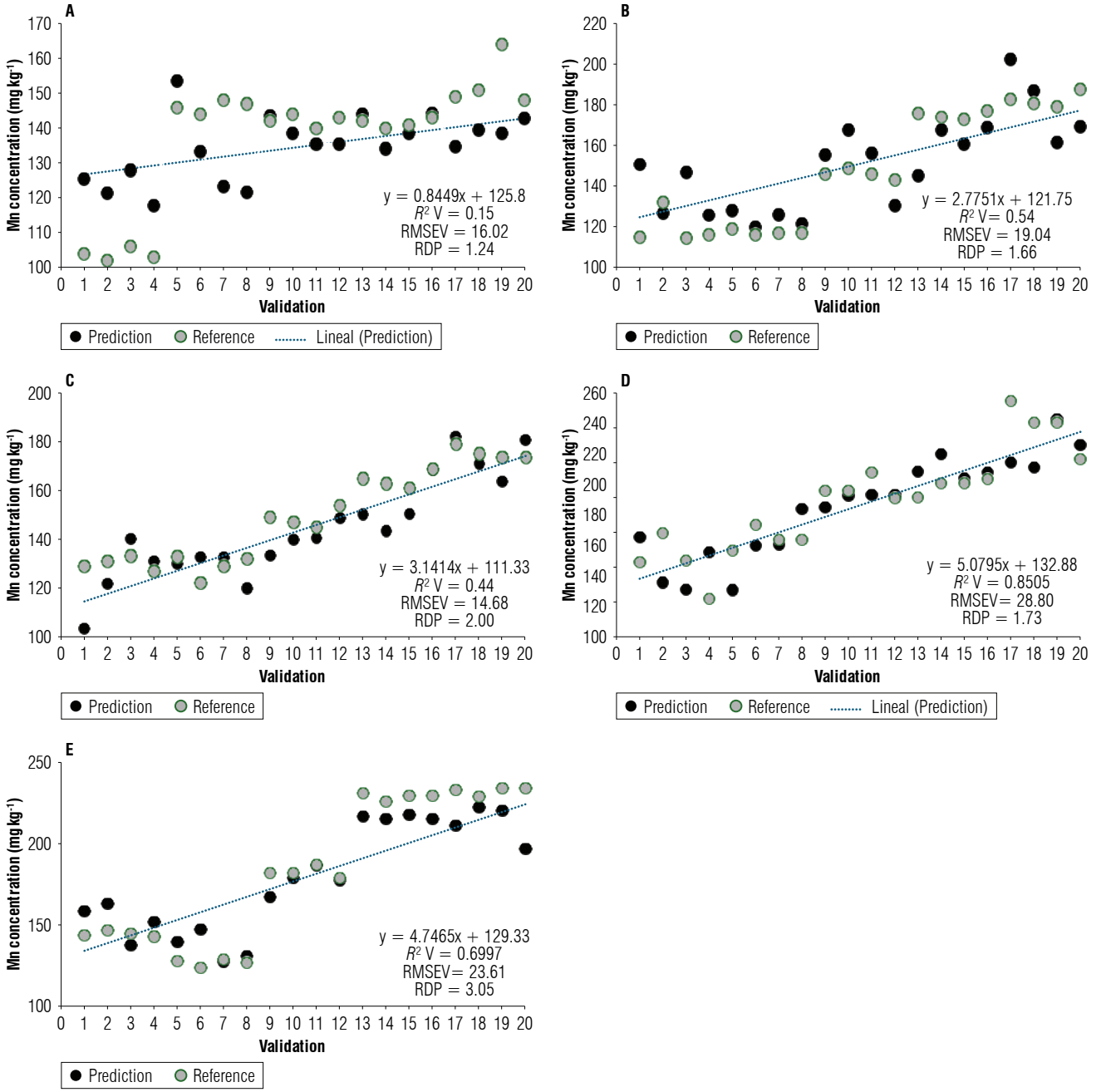

FIGURE 3. Prediction vs reference data in the phenological stages of rose plants: A) palmiche, B) rice, C) chickpea, D) scratch color, and E) straight sepals.

From the results presented, in the palmiche and rice phenological stages, there were no good correlations with the evaluated reflectances, nor good performance of the predictive models. Starting from the chickpea phenological stage, the models showed better performance, with the RN-PLSR model being the best for the chickpea stage, SG-RN-PLSR for the scratch color stage, and Row-PLSR for straight sepals stage.

Figure 4 indicates the spectral regions that had the greatest impact on the predictive models with the best performance for each evaluated phenological stage. For the chickpea phenological stage, where the best-performing model was RN-PLSR (350 nm - 1000 nm), the most relevant regions were 523 nm, 557 nm, 703 nm, and 714 nm. In the scratch color phenological stage, where the best model was SG-RN-PLSR (350 nm - 1800 nm), the key regions were 711 nm, 1341 nm, and 1394 nm. In the straight sepals phenological stage, where the best-performing model was RD-PLSR (350 nm - 2500 nm), the most influential regions were 720 nm, 1420 nm, and 1840 nm. From the chickpea to straight sepals stages, three spectral regions that had the greatest influence on the model performance were around 523 nm, 557 nm and 720 nm.

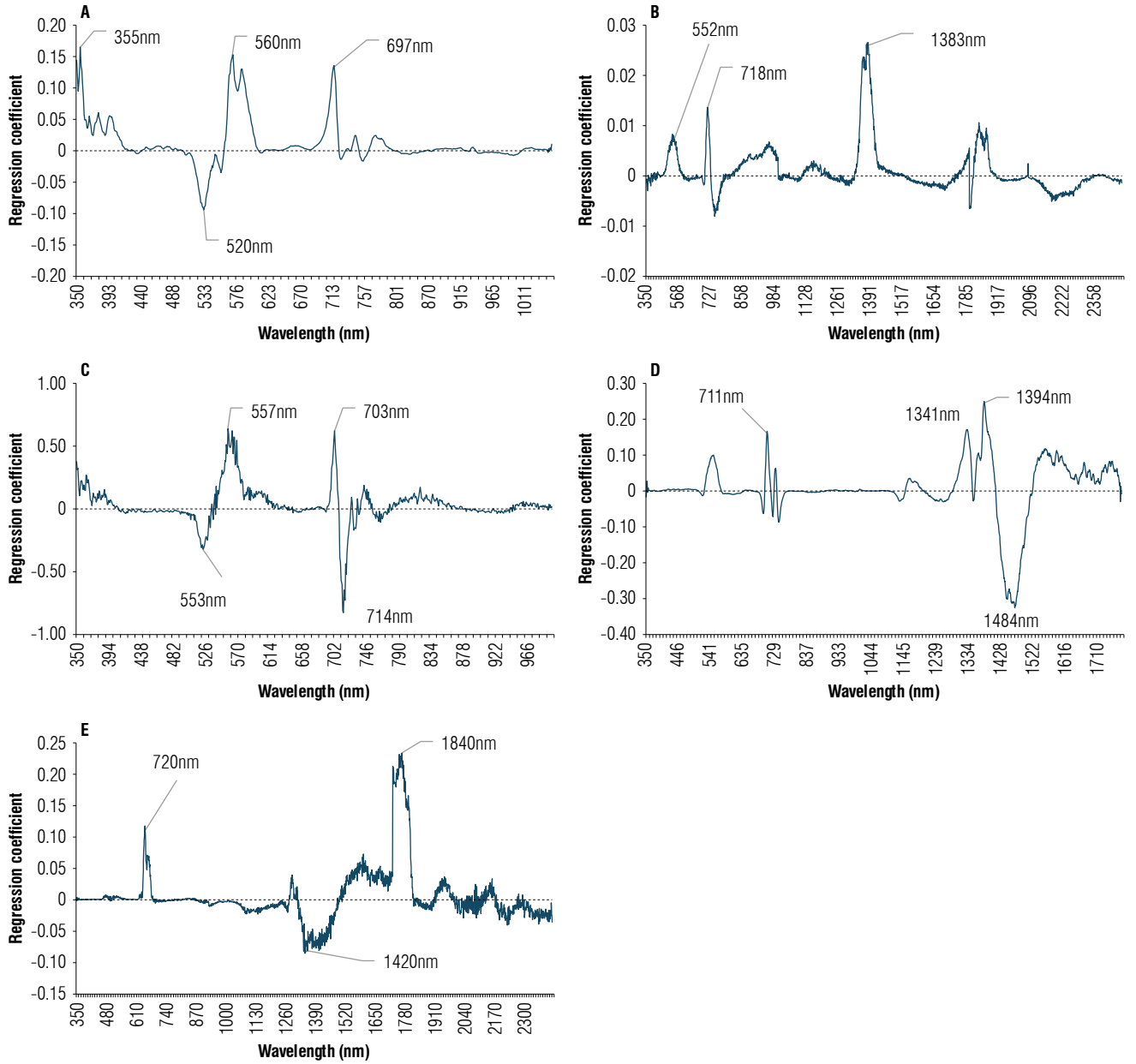

FIGURE 4. Wavelengths with the greatest influence in the predictive models: A) palmiche, B) rice, C) chickpea, D) scratch color, and E) straight sepals.

To determine the confidence of the regressions, an F-test was performed for the selected PLSR models in the phenological stages "chickpea," "scratch color," and "straight sepals". The results are summarized in Table 3. The F-test was conducted with a 95% confidence interval, meaning the significance level is $\alpha = 0.05$. The p-value obtained is less than the significance level α, indicating that the three regression models are statistically significant.

TABLE 3. F-test results.

Phenological stage	Model	DF	F value	*P* value
Chickpea	RN-PLSR	18	67.22	1.73E-04
Scratch color	SG-RN-PLSR	18	39.21	6.62E-03
Straight sepals	RD-PLSR	18	258.00	4.07E-09

From the results presented above, it can be inferred that in the phenological stages of palmiche and rice, no good correlations with the evaluated reflectances were observed, nor did the predictive models perform well according to the metric values. From the phenological stage of chickpea onwards, the models showed better performance, with the RN-PLSR, SG-RN-PLSR, and RD-PLSR models being the most effective. From the phenological stage of rice to straight sepals, three spectral zones were identified, whose reflectances have a greater contribution to the performance of the models: 523 nm, 557 nm, and near 720 nm. These zones are more influential in each sampled period and are key to predicting manganese concentrations in the rose crop.

Figure 5 presents the dual-axis correlations between the predicted values and the actual Mn contents for the selected models in each phenological stage, comparing the regressions using the PLSR and the PCR regression method. The results show that the models that performed better were those using the PLSR method. In the palmiche phenological stage (Fig. 5A), for the same spectral range with the SG-RN techniques, the PLSR model obtained an R^2 of 0.36, while the PCR model reached an R^2 of 0.14. In the rice phenological stage (Fig. 5B), the RD-PLSR model presented an R^2 of 0.63, and the PCR model an R^2 of 0.60. This trend in favor of PLSR was maintained in the subsequent phenological stages.

In chickpea (Fig. 5C), the PLSR model achieved an R^2 of 0.78, while the PCR model obtained an R^2 of 0.46. For the scratch color phenological stage (Fig. 5D), the R^2 value was 0.68 for PLSR, while for PCR it was 0.16. In the straight sepals phenological stage, PLSR presented an R^2 of 0.93, while PCR achieved an R^2 of 0.64. Although in some phenological stages both methods achieved good R^2 values, the PLSR model consistently performed better across all the evaluated phenological stages.

The findings of this study, where PLSR models consistently outperformed PCR in predicting foliar manganese (Mn) concentration in *Rosa* spp., are consistent with previous research across various crops. As reported by Mahajan *et al*. (2021), PLSR yielded better predictions of foliar nutrients in mango compared to PCR and traditional regression approaches. Similar results were observed in oil palm (Santoso *et al*., 2019) and common bean (Boshkovski *et al*., 2020), where PLSR demonstrated robustness, especially when applied alongside spectral preprocessing techniques such as Savitzky-Golay (SG) and range normalization (RN). Unlike PCR, which maximizes variance in the predictor variables without considering the response variable, PLSR optimizes the covariance between both sets, making it ideal for collinear spectral data, such as that obtained through VIS-NIR spectroscopy (Wold *et al*., 2001).

The improved modeling of Mn is particularly relevant, as this nutrient has proven difficult to predict in citrus crops, as noted by Gálvez-Sola *et al*. (2015). In contrast, the present study achieved superior performance metrics during key phenological stages ("straight sepals" and "chickpea"), which may be attributed to the specific optical properties of the rose crop, as well as the experimental design and preprocessing techniques employed. Spectral regions around 523, 557, and 720 nm were consistently important, aligning with findings from other studies (Hu *et al*., 2011; Mahajan *et al*., 2021), further reinforcing their relevance as indicators of nutrient content.

These results are also aligned with the study by Mahajan *et al*. (2024), who combined hyperspectral remote sensing with machine learning algorithms (PLSR-Cubist, SVM, elastic net) to estimate foliar nutrients in cashew. In that study, Mn prediction using PLSR-Cubist was particularly strong, with a coefficient of variation of 21% in the calibration set and a slightly positively skewed distribution, indicating its suitability as a model variable.

Similarly, Acosta *et al*. (2023) reported the effectiveness of PLSR in citrus crops, achieving reliable predictions of macro and micronutrients, with the best results for P, K, and B. In this case, Mn showed optimal and consistent foliar values throughout the crop cycle, which—along with the identification of visible-range wavelengths associated with foliar pigments—supports its diagnostic utility through spectroscopy.

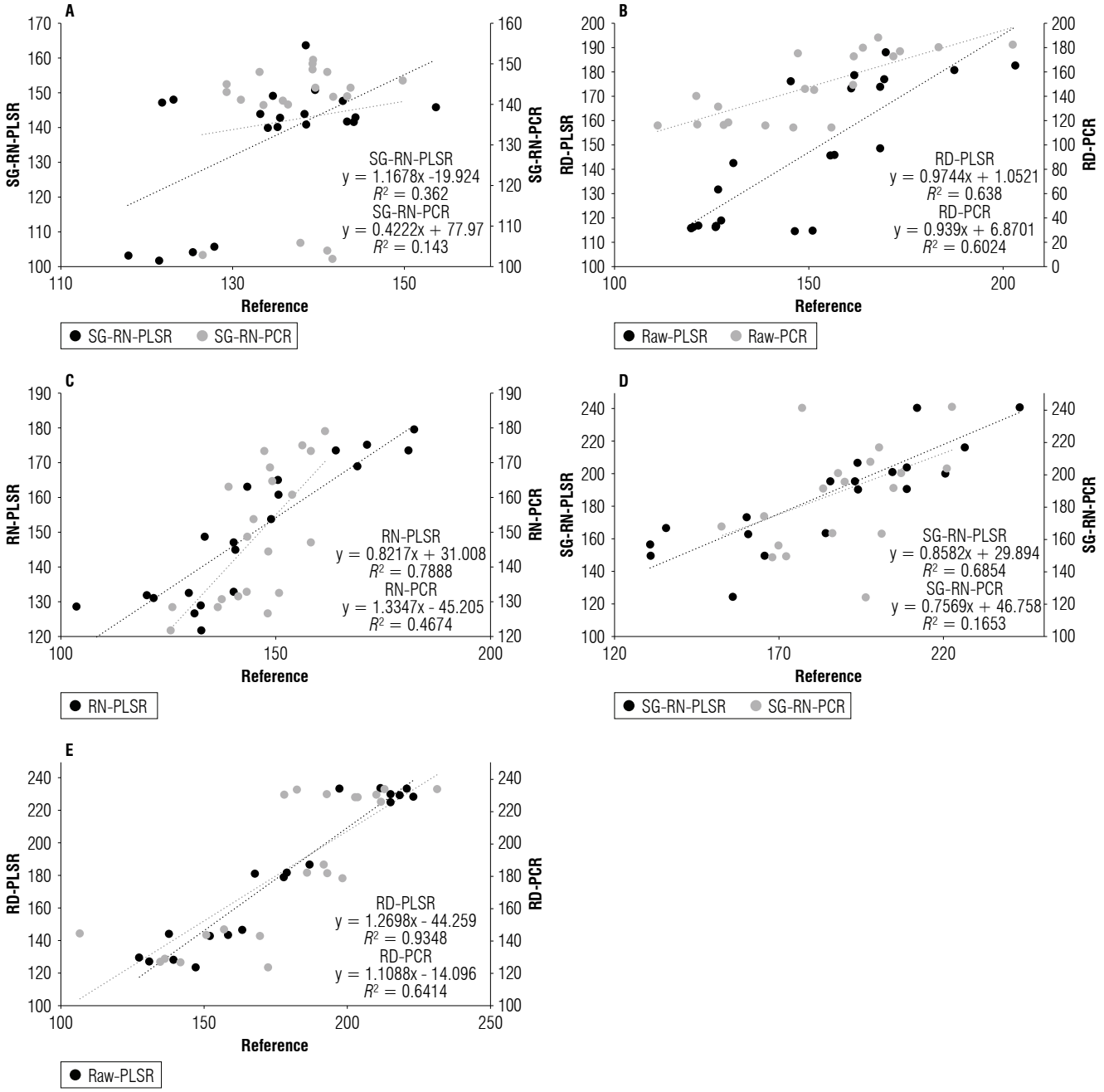

FIGURE 5. Dual-axis correlation comparing the regression techniques PLSR and PCR: A) palmiche, B) rice, C) chickpea, D) scratch color, and E) straight sepals.

In a different but complementary approach, Kusumiyati *et al*. (2022) validated the use of VIS-NIR spectroscopy for estimating nutritional compounds in green cayenne pepper fruits ('Ratuni UNPAD'). Their models achieved high accuracy for carotenoids, water, and capsaicin (RPDs ranging from 1.90 to 2.29), positioning this technique as an efficient, non-destructive alternative for quality control. Finally, studies in Chinese cabbage (*Brassica campestris* L. ssp. Pekinensis 'Norangbom') have shown that VIS-NIR spectroscopy combined with SMLR significantly outperforms conventional sap tests for estimating foliar nitrogen. SMLR produced an R^2 of 0.846 and PLS yielded an R^2 of 0.840 with significantly lower errors (Min *et al*., 2006). These findings support the applicability of similar models

in other species such as *Rosa* spp., where non-destructive Mn detection through PLSR emerges as a promising tool for nutrient monitoring under controlled greenhouse conditions.

Conclusions

This study demonstrated that VIS-NIR spectroscopy, combined with multivariate models such as Partial Least Squares Regression (PLSR), allows for accurate prediction of foliar manganese content in *Rosa* spp. under greenhouse conditions. The models developed—particularly those using Savitzky-Golay smoothing and range normalization—showed robust performance metrics, validating their potential as non-destructive tools for nutritional diagnosis.

The application of this methodology represents an efficient and rapid alternative to conventional foliar analysis, which is especially relevant in highly technical and quality-sensitive crops like roses. The possibility of implementing real-time nutritional monitoring can lead to improved crop management decisions, greater uniformity in floral quality, and reduced laboratory costs.

As a future projection, it is recommended to expand the sample size and validate the models under different environmental conditions and in other rose cultivars. Additionally, hybrid approaches that combine spectral regression with machine learning algorithms could be explored to further enhance prediction accuracy and model adaptability. The results contribute to the advancement of precision agriculture tools in floriculture, with direct application to sustainable rose crop management.

Conflict of interest statement

The authors declare that there is no conflict of interests regarding the publication of this article.

Author's contributions

LJMM was responsible for the conceptual design and objectives of the study; OFM supervised the experiments, managed data collection and maintenance, performed statistical analyses and wrote computer codes, and coordinated the project funding; OFM conducted field and laboratory experiments, as well as created effective visual representations of the data and findings; LJMM and OFM designed and developed the research methodology, including methods and equipment for data collection, and ensured the accuracy and reliability of the results through a rigorous validation process; OFM wrote the initial draft. All authors contributed to the critical review and approved the final version of the manuscript.

Literature cited

Acosta, M., Quiñones, A., Munera, S., Paz, J. M., & Blasco, J. (2023). Rapid prediction of nutrient concentration in citrus leaves using Vis-NIR spectroscopy. *Sensors, 23*(14), Article 6530. https://doi.org/10.3390/s23146530

Arbeláez Torres, G. (1993). La floricultura colombiana de exportación. *Agronomía Colombiana, 10*(1), 5–11. https://revistas.unal.edu.co/index.php/agrocol/article/view/21224

Boshkovski, B., Tzerakis, C., Doupis, G., Zapolska, A., Kalaitzidis, C., & Koubouris, G. (2020). Relationships of spectral reflectance with plant tissue mineral elements of common bean (*Phaseolus vulgaris* L.) under drought and salinity stresses. *Communications in Soil Science and Plant Analysis*, *51*(5), 675–686. https://doi.org/10.1080/00103624.2020.1729789

Franco Montoya, O. H., & Martínez Martínez, L. J. (2024). Relationship between spectral response and manganese concentrations for assessment of the nutrient status in rose crop. *Agronomía Colombiana, 42*(2), Article e110294. https://doi.org/10.15446/agron.colomb.v42n2.110294

Gálvez-Sola, L., García-Sánchez, F., Pérez-Pérez, J. G., Gimeno, V., Navarro, J. M., Moral, R., Martínez-Nicolás, J. J., & Nieves, M. (2015). Rapid estimation of nutritional elements on citrus leaves by near infrared reflectance spectroscopy. *Frontiers in Plant Science, 6*, Article 571. https://doi.org/10.3389/fpls.2015.00571

Ghosh, S., Prasanna, V. L., Sowjanya, B., Srivani, P., Alagaraja, M., & Banji, D. (2013). Inductively coupled plasma–optical emission spectroscopy: A review. *Asian Journal of Pharmaceutical Analysis*, *3*(1), 24–33. https://ajpaonline.com/HTMLPaper.aspx?Journal=Asian%20Journal%20of%20Pharmaceutical%20Analysis;PID=2013-3-1-6

Hariyadi, B. W., Nizak, F., Nurmalasari, I. R., & Kogoya, Y. (2019). Effect of dose and time of NPK fertilizer application on the growth and yield of tomato plants (*Lycopersicum esculentum* Mill). *Agricultural Science, 2*(2), 101–111. http://agriculturalscience.unmerbaya.ac.id/index.php/agriscience/article/view/26

Huber, S., Kneubühler, M., Psomas, A., Itten, K., & Zimmermann, N. E. (2008). Estimating foliar biochemistry from hyperspectral data in mixed forest canopy. *Forest Ecology and Management, 256*(3), 491–501. https://doi.org/10.1016/j.foreco.2008.05.011

Hu, J., He, D., & Yang, P. (2011). Study on plant nutrition indicator using leaf spectral transmittance for nitrogen detection. In D. Li, Y. Liu, & Y. Chen (Eds.), *Computer and computing technologies in agriculture IV: 4th IFIP TC 12 Conference, CCTA 2010* (Vol. 347, pp. 504–513). Springer. https://doi.org/10.1007/978-3-642-18369-0_60

Humphries, J. M., Stangoulis, J. C., & Graham, R. D. (2006). Manganese. In A. V. Barker, & D. J. Pilbeam (Eds.), *Handbook of plant nutrition* (pp. 351–374). CRC Press. https://doi.org/10.1201/9781420014877

ICA – Instituto Colombiano Agropecuario. (2024). Con 700 millones de tallos, Colombia aporta variedad, color y belleza a la celebración de San Valentín. https://www.ica.gov.co/noticias/ica-colombia-exporta-flores-san-valentin-2024

Kusumiyati, K., Putri, I. E., Hamdani, J. S., & Suhandy, D. (2022). Real-time detection of the nutritional compounds in green

'Ratuni UNPAD' cayenne pepper. *Horticulturae, 8*(6), Article 554. https://doi.org/10.3390/horticulturae8060554

Lê Cao, K. A., Rossouw, D., Robert-Granié, C., & Besse, P. (2008). Sparse PLS: Variable selection when integrating omics data. *Statistical Applications in Genetics and Molecular Biology, 7*(1), Article 35. https://hal.science/hal-00300204v1/file/sPLS.pdf

Lee, W., Searcy, S. W., & Kataota, T. (2000). Assessing nitrogen stress in corn varieties of varying color citrus. *ASAE Meeting Presentation, Paper No. 99-3034*, 1–24. https://www.researchgate.net/publication/2455515

Liang, S. (2005). *Quantitative remote sensing of land surfaces*. John Wiley & Sons. https://onlinelibrary.wiley.com/doi/book/10.1002/047172372X

Mahajan, G. R., Das, B., Kumar, P., Murgaokar, D., Patel, K., Desai, A., Morajkar, S., Kulkarni, R. M., & Gauns, S. (2024). Spectroscopy-based chemometrics combined machine learning modeling predicts cashew foliar macro- and micronutrients. *Spectrochimica Acta Part A: Molecular and Biomolecular Spectroscopy, 320*, Article 124639. https://doi.org/10.1016/j.saa.2024.124639

Mahajan, G. R., Das, B., Murgaokar, D., Herrmann, I., Berger, K., Sahoo, R. N., Patel, K., Desai, A., Morajkar, S., & Kulkarni, R. M. (2021). Monitoring the foliar nutrients status of mango using spectroscopy-based spectral indices and PLSR-combined machine learning models. *Remote Sensing, 13*(4), Article 641. https://doi.org/10.3390/rs13040641

Mevik, B. H., & Wehrens, R. (2007). The PLS package: Principal component and partial least squares regression in R. *Journal of Statistical Software, 18*, 1–23. https://doi.org/10.18637/jss.v018.i02

Min, M., Lee, W. S., Kim, Y. H., & Bucklin, R. A. (2006). Nondestructive detection of nitrogen in Chinese cabbage leaves using VIS–NIR spectroscopy. *HortScience*, *41*(1), 162–166. https://doi.org/10.21273/HORTSCI.41.1.162

Rashed, M. H., Hoque, T. S., Jahangir, M. M. R., & Hashem, M. A. (2019). Manganese as a micronutrient in agriculture: Crop requirement and management. *Journal of Environmental Science and Natural Resources, 12*(1–2), 225–242. https://doi.org/10.3329/jesnr.v12i1-2.52040

Ruppenthal, V., & Castro, A. M. C. (2005). Efeito do composto de lixo urbano na nutrição e produção de gladíolo. *Revista Brasileira de Ciência do Solo*, *29*, 145–150. https://doi.org/10.1590/S0100-06832005000100016

Santos, E. F., Santini, J. M. K., Paixão, A. P., Furlani Júnior, E., Lavres, J., Campos, M., & Reis, A. R. (2017). Physiological highlights of manganese toxicity symptoms in soybean plants: Mn toxicity responses. *Plant Physiology and Biochemistry, 113*, 6–19. https://doi.org/10.1016/j.plaphy.2017.01.022

Santoso, H., Tani, H., Wang, X., & Segah, H. (2019). Predicting oil palm leaf nutrient contents in Kalimantan, Indonesia by measuring reflectance with a spectroradiometer. *International Journal of Remote Sensing, 40*(19), 7581–7602. https://doi.org/10.1080/01431161.2018.1516323

Wold, S., Sjöström, M., & Eriksson, L. (2001). PLS-regression: A basic tool of chemometrics. *Chemometrics and Intelligent Laboratory Systems, 58*(2), 109–130. https://doi.org/10.1016/S0169-7439(01)00155-1

Yu, E., Zhao, R., Cai, Y., Huang, J., Li, C., Li, C., Mei, L., Bao, L., Chen, J., & Zhu, S. (2019). Determination of manganese content in cottonseed meal using near-infrared spectrometry and multivariate calibration. *Journal of Cotton Research*, *2*, Article 12. https://doi.org/10.1186/s42397-019-0030-5